ORIGINAL ARTICLE

Histometric Analysis of Skin-Radiofrequency Interaction Using a Fractionated Microneedle Delivery System

ZHENLONG ZHENG, MD, PHD,*† BONCHEOL GOO, MD,‡ DO-YOUNG KIM, MD,* JIN-SOO KANG, MD,§ AND SUNG BIN CHO, MD, PHD*§

BACKGROUND Fractionated microneedle radiofrequency (RF) devices have been reported to be effective in treatment of various dermatologic disorders.

OBJECTIVES To analyze histometric changes in skin-RF interactions using a fractionated microneedle delivery system.

MATERIALS AND METHODS RF energies were delivered using a fractionated microneedle device to an in vivo minipig model with penetration depths of 0.5, 1.0, 1.5, 2.0, 2.5, and 3.5 mm; RF conduction times of 20, 50, 100, and 1,000 ms; and energy levels of 5.0, 10.0, 20.0, 25.0, 37.5, and 50.0 V.

RESULTS Immediately after treatment, skin samples showed that the RF-induced coagulated columns in the dermis formed a cocoon-shaped zone of sublative thermal injury. Four days after the treatment, skin specimens demonstrated reepithelialization, and the dermal RF-induced coagulated columns showed mixed cellular infiltration, neovascularization, and granulation tissue formation. Microneedle depth and RF conduction times, but not energy level, significantly affected histometric values of RF-induced dermal coagulation. Microneedle RF treatment affected adnexal structures by coagulating follicular epithelium and perifollicular structures.

CONCLUSIONS Our data may be of use as an essential reference for choosing RF parameters in treatment of various skin conditions.

The authors have indicated no significant interest with commercial supporters.

Radiofrequency (RF) devices with fractionated delivery systems are reported to be clinically effective in treating various dermatologic conditions, including wrinkles, acne scars, enlarged pores, and acne vulgaris.[1–4] Water, dermal microvasculature, collagen, and melanin absorb RF energy to produce bulk heating on the dermis, with secretion of cellular mediators and growth factors related to wound healing.[4,5] Fractionated delivery of RF energy facilitates safer treatment of lesions, using higher energy in a noncontiguous pattern, than other fractional lasers.[6] A fractionated RF system creates a pyramid-shaped zone of thermal injury, which is referred to as sublative injury, whereas ablative fractional lasers produce a conical zone of thermal injury, which is widest in the epidermis and narrower in the dermis.[2,6]

Hantash and colleagues[5] reported on a microneedle-assisted fractional bipolar RF delivery system, which allowed for precise depth control in the dermis and epidermal preservation. Several fractionated microneedle RF devices have been introduced, equipped with five linear bipolar needle pairs, twenty-five 32-G needles in a 1-cm^2 disposable tip, or forty-nine 32- to 34-G needles in a 1-cm^2

Department of Dermatology and Cutaneous Biology Research Institute, Yonsei University College of Medicine, Seoul, Korea; †Department of Dermatology, Yanbian University Hospital, Yanji, China; ‡Clinique L, Goyang, Korea; §Kangskin Clinic, Seoul, Korea

ISSN: 1076-0512 • Dermatol Surg 2013;1–8 • DOI: 10.1111/dsu.12411

disposable tip with or without insulation.[1,4,5,7] In previous reports, pretreatment impedance value and lesion temperature were evaluated to optimize RF parameters according to the characteristics of target tissues.[5,7] The authors suggested that RF parameters can be more accurately determined by monitoring lesion temperature and time at temperature than power.[5,7]

Other reports have demonstrated the clinical efficacy of fractionated microneedle RF devices based on the power of RF energy,[1,4] but the absence of reference data with detailed skin-RF interactions prevents practitioners from predicting therapeutic efficacy or side effects of RF devices. Therefore, in the present study, we investigated the skin-RF interactions of a fractionated microneedle RF device in accordance with various energy settings using a minipig model. Treated skin samples obtained from two female minipigs, which have structural and functional similarities to those of human skin, were histometrically analyzed.

Materials and Methods

In vivo Minipig Model

After permission was granted from the ethics committee of the Yonsei University Institutional Animal Care and Use Committee, the following protocol was performed. Two female 3-month-old SPF minipigs weighing 8.42 and 8.48 kg were used in this protocol. General anesthesia was induced by means of an intramuscular bolus injection of tiletamine and zolazepam (6 mg/kg) and atropine (0.05 mg/kg). Endotracheal intubation was performed, and a ventilator was connected. Lungs were ventilated with oxygen, and anesthesia was maintained using 1.8% isoflurane. Intravenous hydration with normal saline was maintained through a superficial auricular vein (25 mL/h).

Fractionated Microneedle RF Device and Treatment Protocol

The minipigs were treated in a single session of a fractionated microneedle RF (INFINI; Lutronic Corporation, Goyang, Korea). The device was equipped with a hand-piece and a 1-cm^2 disposable microneedle tip, which had 49 proximally insulated 34-G microneedle electrodes. The minipigs were shaved using an electrical cutter, and the skin was marked with dot-ink to define 1-cm^2 grids reflecting each treatment parameter; each grid was at least 1 cm from the others to minimize RF effects on other treatment areas. The operative field was cleansed with a mild soap and 70% alcohol. The RF energies were then delivered to each grid with

TABLE 1. Representative Treatment Parameters and Histometric Analyses of Skin-Radiofrequency (RF) Interaction

		RF Conduction Time (ms)					
Microneedle Depth (mm)	*Energy Level (V)*	*50*		*100*		*1,000*	
		Height (μm)	*Width (μm)*	*Height (μm)*	*Width (μm)*	*Height (μm)*	*Width (μm)*
		Zone of Thermal Injury, Maximum ± Standard Deviation					
1.5	10.0	219.9 ± 40.8	151.4 ± 16.2	414.7 ± 38.4	220.9 ± 7.8	648.9 ± 15.1	437.0.±6.7
	25.0	245.6 ± 7.8	135.0 ± 6.6	385.9 ± 4.8	192.2 ± 4.4	578.5 ± 5.6	388.4 ± 4.2
	50.0	360.3 ± 5.4	194.7 ± 2.6	384.3 ± 16.2	232.7 ± 7.1	607.0 ± 7.1	395.0 ± 8.2
2.5	10.0	364.8 ± 11.0	136.0 ± 7.3	526.9 ± 11.2	262.5 ± 11.8	1009.0 ± 13.5	717.9 ± 11.2
	25.0	660.4 ± 10.1	205.9 ± 13.8	800.6 ± 26.3	443.6 ± 13.8	1169.8 ± 2.9	718.9 ± 9.5
	50.0	613.1 ± 4.5	311.5 ± 3.4	850.3 ± 11.2	502.8 ± 3.9	1039.1 ± 17.1	602.9 ± 7.7
3.5	10.0	384.2 ± 6.2	128.9 ± 8.7	529.1 ± 17.0	225.4 ± 8.6	1122.7 ± 18.7	919.8 ± 5.8
	25.0	682.1 ± 14.2	270.5 ± 4.6	1121.6 ± 15.2	444.4 ± 6.7	1258.6 ± 2.9	835.8 ± 4.6
	50.0	1084.8 ± 16.9	399.4 ± 9.5	1034.2 ± 11.8	571.6 ± 10.1	1361.7 ± 20.8	685.2 ± 8.7

microneedle depths of 1.5, 2.5, and 3.5 mm; RF conduction times of 20, 50, 100, and 1,000 m; and energy levels of 5.0, 10.0, 20.0, 25.0, 37.5, and 50.0 V.

Histometric Evaluation

The minipig skin samples for each parameter were obtained immediately, 4 days, and 2 weeks after the microneedle RF treatments; fixed in 10% buffered formalin; and embedded in paraffin. Twenty to 30 serial pieces of 5-μm-thick skin sections were subsequently prepared for histometric evaluation of maximum skin-RF interaction for each condition. The sections were stained with hematoxylin and eosin, and the mean maximum height and width of RF-induced coagulated columns were determined (ImageJ 1.43u; National Institutes of Health, Bethesda, MD).[8] Verhoeff-van Gieson and Masson trichrome stains were also performed.

Statistical Analysis

Significant differences were evaluated according to parametric criteria after the normality test using the Kolmogorov-Smirnov test. Analysis of variance with

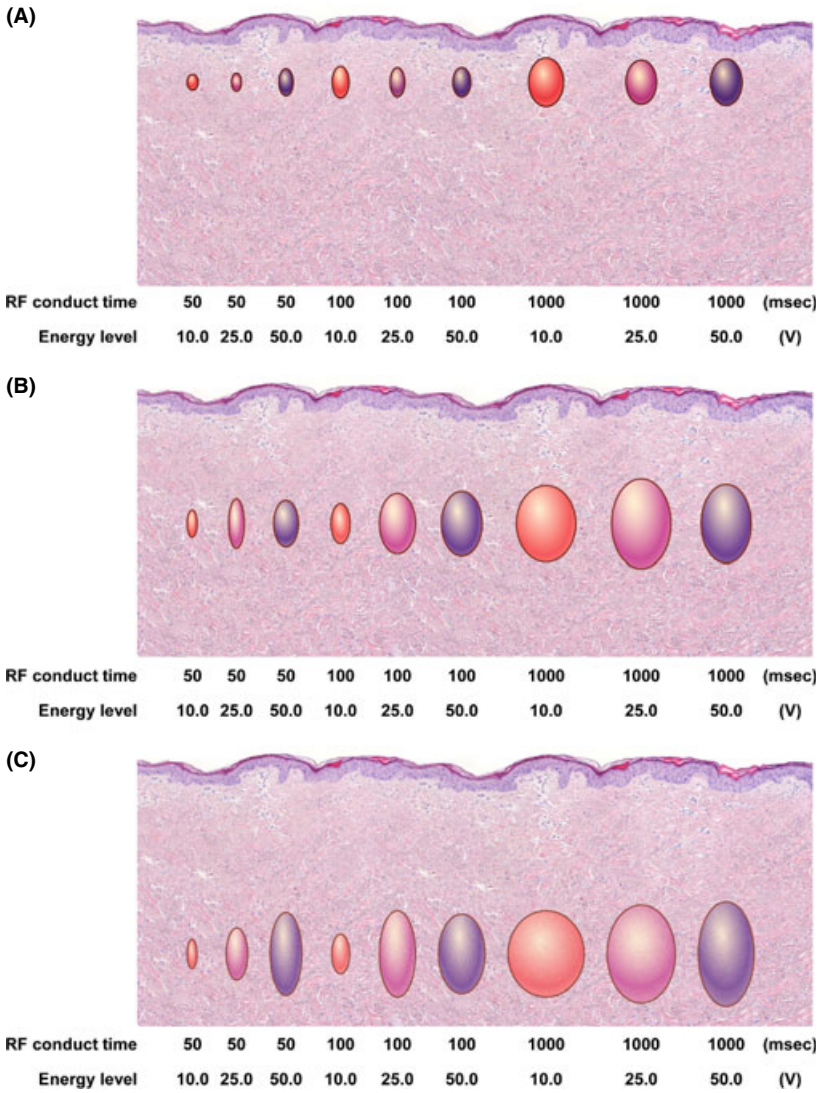

Figure 1. Schematic view of radiofrequency (RF)-skin interaction after microneedle fractionated RF treatment with representative treatment parameters. Microneedle depths of (A) 1.5, (B) 2.5, and (C) 3.5 mm.

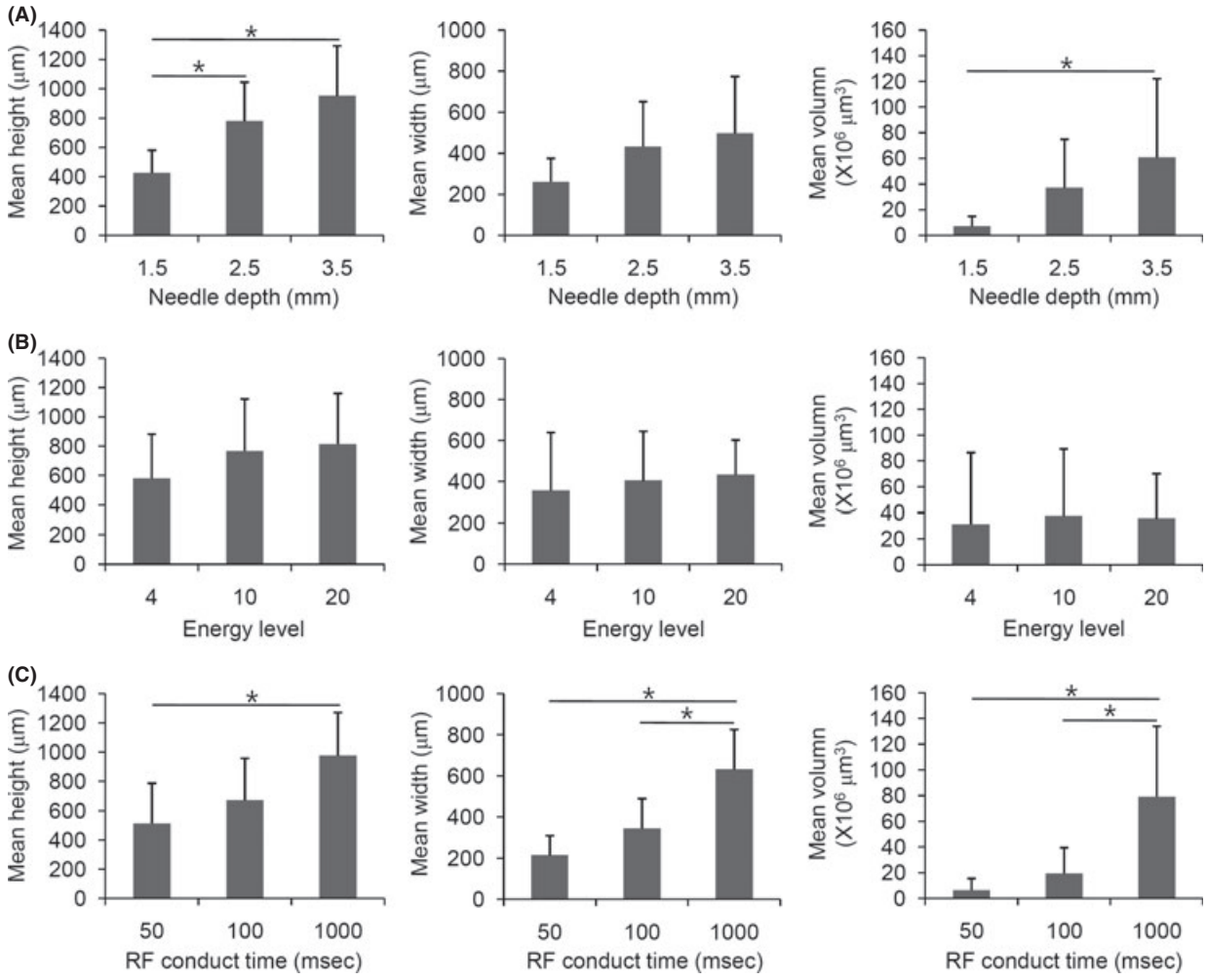

Figure 2. Effects of radiofrequency (RF) treatment parameters, (A) microneedle depth, (B) energy level, and (C) RF conduction time on the height, width, and volume of coagulated columns. *$p < .05$.

Bonferroni post hoc test was used to analyze the effects of RF treatment parameters on cutaneous histometric and volumetric changes. The results with $P < .05$ were considered statistically significant. All analyses were performed using SAS version 9.2 (SAS Institute, Inc., Cary, NC).

Results

Histometric Changes

Histometric changes of skin-RF interaction with representative treatment parameters are summarized in Table 1 and illustrated in Figure 1. The depths of the microneedles ($p = .001$) and the RF conduction times ($p = .007$) but not energy level ($p > .05$) significantly affected post-therapy mean height of the coagulated columns (Figure 2A). RF conduction time also significantly changed Mean width of the zone of thermal injury ($p < .001$) but not the depths of the microneedles ($p > .05$) or energy level ($p > .05$) (Figure 2B). On the supposition that microneedle RF treatment created conical diamond-shaped tissue coagulation in the dermis, the depths of microneedles ($p = .04$) and RF conduction time ($p < .001$) but not energy level ($p > .05$) significantly affected the calculated volume (Figure 2C). Depending on the energy level, various degrees of tissue destruction were apparent on Verhoeff-van

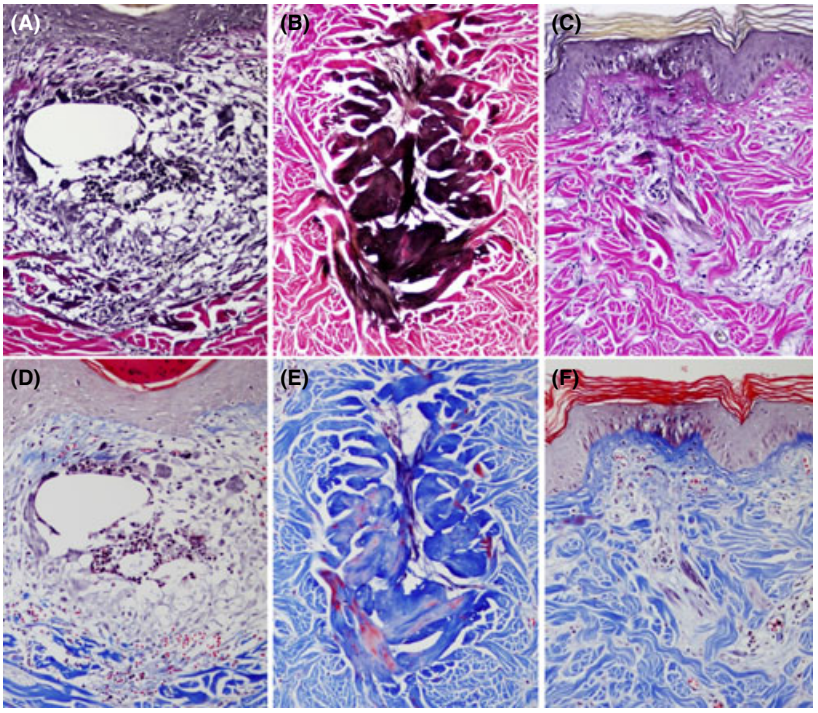

Figure 3. Minipig skin samples (A, D) immediately after fractionated microneedle radiofrequency (RF) treatment with microneedle depths of 1.5 mm, energy level of 10.0 V, and RF conduction time of 50 ms; (B, E) immediately and (C, F) 4 days after fractionated microneedle RF treatment with microneedle depths of 1.5 mm, energy level of 25.0 V, and RF conduction time of 100 ms (A–C, Verhoeff-van Gieson stain; D–F, Masson trichrome stain; original magnification ×200).

Gieson and Masson trichrome stains. Delivery of RF at lower energy levels produced obvious coagulated columns (Figure 3A,D), but dermal structures were preserved more than in minipig skin treated with RF at higher energy levels (Figure 3B,E).

Wound Healing Process

Immediately after the treatment, the skin samples showed that the RF-induced coagulated columns in the dermis formed a cocoon-shaped zone of sublative thermal injury (Figure 4A,D). The epidermis was also affected when the RF was delivered upward from the inserted tip, particularly with 1.5-mm microneedle depth. Four days after the treatment, the skin specimens showed reepithelialization and dermal RF-induced coagulated columns with mixed cellular infiltration, neovascularization, and granulation tissue formation (Figure 4B,E). Proliferation of fibroblasts, elastogenesis, and neocollagen formation were also noted in the treated dermis (Figure 3C,F). Two weeks after the treatment, activated fibroblasts and inflammatory cells were present, and neocollagen replaced coagulated columns (Figure 4C,F). Combined treatment with different device settings produced RF-induced coagulated columns in the dermis at different levels (Figure 5).

Effects of Microneedle RF on Adnexal Structures

The serially sectioned biopsy specimens were reviewed to investigate the effects of microneedle RF energy on adnexal structures, especially the hair follicles. Among them, skin specimens obtained immediately after the microneedle RF treatment with a microneedle depth of 3.5 mm, energy level of 50.0 V, and RF conduction time of 50 ms demonstrated a zone of coagulated follicular epithelium and perifollicular structures, which disrupted the structural integrity of hair follicles (Figure 6A). When the RF was delivered with a microneedle

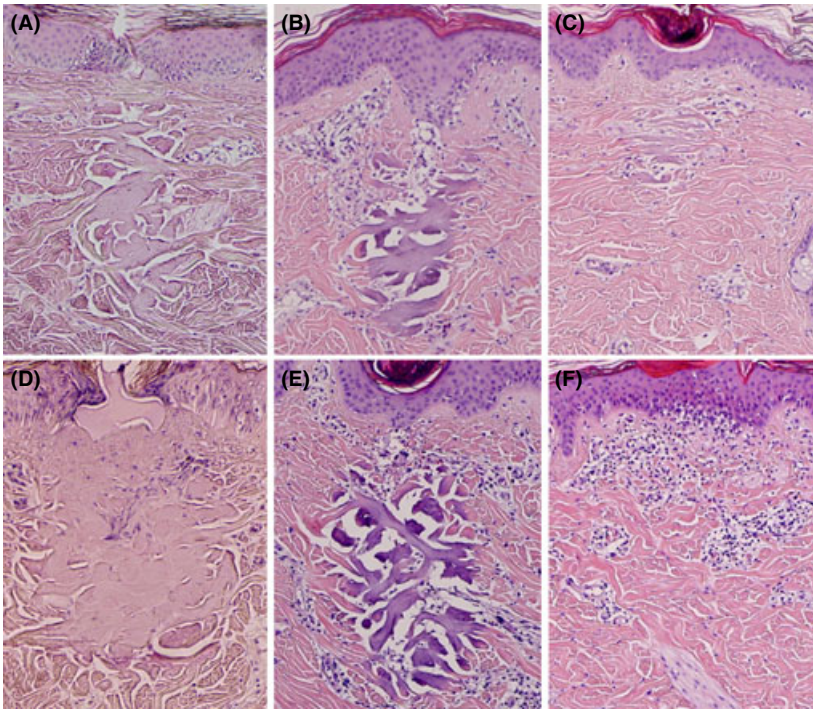

Figure 4. Histologic features of minipig skin samples (A, D) immediately and (B, E) 4 days, and (C, F) 2 weeks after fractionated microneedle radiofrequency (RF) treatment with microneedle depths of 1.5 mm and energy level of 25.0 V; RF conduction time of (A–C) 20 ms and (D–F) 100 ms (hematoxylin and eosin stain; original magnification ×100).

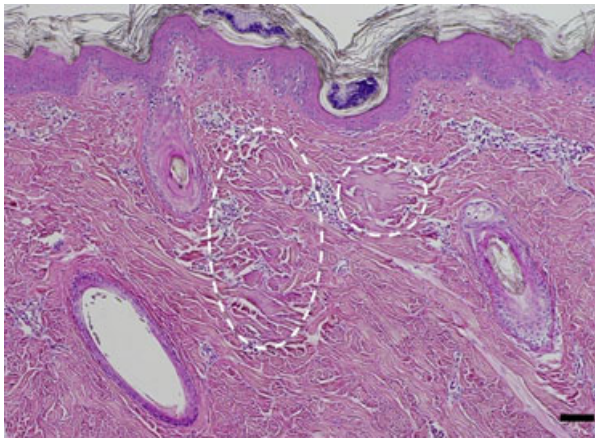

Figure 5. Fractionated microneedle radiofrequency (RF) treatment with the combined parameters of (right white dotted oval) microneedle depth of 2.0 mm, energy level of 10.0 V, and RF conduction time of 50 ms and (left white dotted oval) microneedle depth of 3.5 mm, energy level of 20.0V, and RF conduction time of 100 ms. The skin samples were obtained 1 week after the treatment (hematoxylin and eosin stain; original magnification ×100; bar = 100 μm).

depth of 3.5-mm, energy level of 25.0 V, and RF conduction time of 100 ms, the follicular epithelium and perifollicular structures were coagulated, but the structural integrity of hair follicles was preserved (Figure 6B).

Four days after microneedle RF treatment with a microneedle depth of 1.5 mm, energy level of 25.0 V, and RF conduction time of 20 ms, coagulated follicular epithelium demonstrated reepithelialization and mixed cellular infiltration, neovascularization, and granulation tissue formation around the hair follicles, with preserved follicular structural integrity (Figure 6C).

Discussion

The present study demonstrated the skin-RF interactions of a fractionated microneedle RF device according to various energy settings using a minipig model. Previous investigations demonstrated that microneedle RF-induced tissue responses with denatured collagen were found within the reticular dermis after insertion of five pairs of electrodes through the epidermis into the skin at a distance of

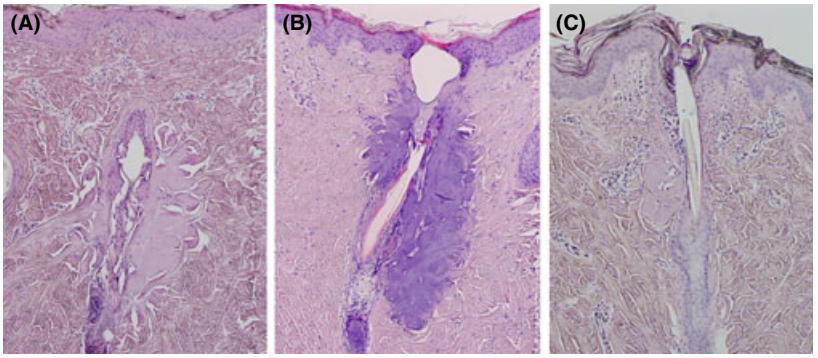

Figure 6. Histologic changes of hair follicles after fractionated microneedle radiofrequency (RF) treatment. (A) Immediately after the microneedle RF treatment with microneedle depth of 3.5 mm, energy level of 50.0 V, and RF conduction time of 50 ms. (B) Immediately after the microneedle RF treatment with microneedle depth of 3.5 mm, energy level of 25.0 V, and RF conduction time of 100 ms. (C) Four days after the microneedle RF treatment with microneedle depth of 1.5 mm, energy level of 25.0 V, and RF conduction time of 20 ms (hematoxylin and eosin stain; original magnification ×100).

6 mm at a 20° angle.[5,7] Fractionated RF treatments reportedly induced an active dermal remodelling process, with expression of heat shock proteins (HSPs), metalloproteinases (MMPs), and inflammatory cytokines, including HSP47, HSP72, interleukin-1β, tumor necrosis factor alpha, tumor growth factor beta, MMP-1, MMP-3, MMP-9, and MMP-13.[7] RF-induced neoelastogenesis and neocollagenesis have also been noted in RF thermal zones within 1 month after treatment.[7]

In this study, we used a fractionated microneedle RF device with a hand piece and a 1-cm^2 disposable microneedle tip with 49 proximally insulated microneedle electrodes. Microneedles penetrated the skin perpendicularly and delivered RF to the target tissue, generating 49 coagulated columns. Although shorter procedure time has been shown to reduce post-treatment bleeding and oozing and result in more-rapid recovery,[9] pretreatment impedance value and lesion temperature have yet to be monitored in real time according to the characteristics of target tissues. Nevertheless, organized data reflecting parameter-dependent skin-RF interactions is needed to help practitioners predict clinical outcomes and avoid side effects of RF devices. Moreover, overlapped treatments involve a high risk of causing bulk heat damage to the treated tissues as a result of heat stacking. Accordingly, we histologically demonstrated a combination of RF device settings with different microneedle depths that can be used to more effectively and safely provide multilayered zones of thermal injury.

Electric currents that RF devices generate produce thermal effects through resistance in the dermis, resulting in skin rejuvenation. Microneedle depth–dependent histometric changes in the areas of sublative thermal injury result from different impedance values of dermal structures. Significant differences in impedance and permittivity between the papillary dermis, reticular dermis, and subcutaneous fat layers have been demonstrated.[5] Typically, lower impedance and higher permittivity of the superficial papillary dermis show a smaller but more highly concentrated zone of thermal injury caused by RF treatment than in the reticular dermis or subcutaneous fat layers.[5,10,11] The present study found that the depths of the microneedles and the RF conduction times, but not energy level, significantly affected histometric values of RF-induced dermal coagulation. It may be that energy levels are closely related to intensity of thermal injury rather than extent of energy delivery.

RF energy delivered to the skin spares adnexal structures and adipose tissue.[5] Periadnexal collagen and interstitial collagen have been shown to be coagulated with RF treatment, whereas blood vessels, sweat glands, sebaceous glands, hair follicles,

and fat tissue are well preserved.[5] In the present study, we found that microneedle RF treatment affected terminal hair follicles by coagulating follicular epithelium and perifollicular structures with or without disrupting the structural integrity of hair follicles depending on the treatment parameters. During the wound healing process, the coagulated follicular structures demonstrated reepithelialization and mixed cellular infiltration, neovascularization, and granulation tissue formation around the hair follicle, which preserved follicular structural integrity. Nevertheless, although serially sectioned biopsy specimens treated with various parameters were reviewed in our study, small adnexal structures other than the terminal hair follicles, especially sweat glands and sebaceous glands, were not fully evaluated.

Although RF-induced histometric changes in minipig skin do not exactly reflect that of human facial skin, the therapeutic efficacy and safety of laser and light devices for the skin have been investigated using minipig models. We believe that our data can be used as an essential reference for choosing RF parameters in treatment of various skin conditions by analyzing histometric skin-RF interactions according to the representative treatment parameters.

Acknowledgments

We thank Hye Sun Lee, PhD (Biostatistician, Biostatistics Collaboration Unit, Yonsei University College of Medicine, Seoul, Korea) for her help with the statistical analyses and Dong-Su Jang (Medical Illustrator, Medical Research Support Section, Yonsei University College of Medicine, Seoul, Korea) for his help with the figures.

References

1. Cho SI, Chung BY, Choi MG, Baek JH, et al. Evaluation of the clinical efficacy of fractional radiofrequency microneedle treatment in acne scars and large facial pores. Dermatol Surg 2012;38:1017–24.
2. Peterson JD, Palm MD, Kiripolsky MG, Guiha IC, et al. Evaluation of the effect of fractional laser with radiofrequency and fractionated radiofrequency on the improvement of acne scars. Dermatol Surg 2011;37:1260–7.
3. Man J, Goldberg DJ. Safety and efficacy of fractional bipolar radiofrequency treatment in Fitzpatrick skin types V–VI. J Cosmet Laser Ther 2012;14:179–83.
4. Lee SJ, Goo JW, Shin J, Chung WS, et al. Use of fractionated microneedle radiofrequency for the treatment of inflammatory acne vulgaris in 18 Korean patients. Dermatol Surg 2012;38:400–5.
5. Hantash BM, Renton B, Berkowitz RL, Stridde BC, et al. Pilot clinical study of a novel minimally invasive bipolar microneedle radiofrequency device. Lasers Surg Med 2009;41:87–95.
6. Brightman L, Goldman MP, Taub AF. Sublative rejuvenation: experience with a new fractional radiofrequency system for skin rejuvenation and repair. J Drugs Dermatol 2009;8:S9–13.
7. Hantash BM, Ubeid AA, Chang H, Kafi R, et al. Bipolar fractional radiofrequency treatment induces neoelastogenesis and neocollagenesis. Lasers Surg Med 2009;41:1–9.
8. Collins TJ. ImageJ for microscopy. Biotechniques 2007;43:25–30.
9. Cho SB, Lee SJ, Kang JM, Kim YK, et al. The treatment of burn scar-induced contracture with the pinhole method and collagen induction therapy: a case report. J Eur Acad Dermatol Venereol 2008;22:513–4.
10. Emilia del Pino PM, Rosado RH, Azuela A, Graciela GM, et al. Effect of controlled volumetric tissue heating with radiofrequency on cellulite and the subcutaneous tissue of the buttocks and thighs. J Drugs Dermatol 2006;5:714–22.
11. Trelles MA, van der Lugt C, Mordon S, Ribé A, et al. Histological findings in adipocytes when cellulite is treated with a variable-emission radiofrequency system. Lasers Med Sci 2010;25:191–5.

Address correspondence and reprint requests to: Sung Bin Cho, MD, PhD, Department of Dermatology and Cutaneous Biology Research Institute, Yonsei University College of Medicine, 50 Yonsei-ro, Seodaemun-gu, 120–752 Seoul, Korea, or e-mail: drsbcho@gmail.com